Research Laboratory) for directing our attention toward the spectral spin-diffusion experiment, for a preprint of his manuscript, and for helpful discussions. Thanks are also due to Drs. David Lathrop and Regina Francisco and to Ms. Deanna Franke for help with the data analysis. Acknowledgment is made to the donors of the Petroleum Research Fund, administered by the American Chemical Society, and to the National Science Foundation (Grant DMR 89-13738) for financial support of this research.

Molecular Orbital Studies of the Structure and Reactivity of Model Substrate Intermediates in the Deacylation of the Cysteine Protease Papain

Gregory D. Duncan,[†,‡] Carol P. Huber,[§] and William J. Welsh*[,†]

Contribution from the Department of Chemistry, University of Missouri—St. Louis, St. Louis, Missouri 63121, and National Research Council of Canada, Ottawa, Ontario, Canada K1A OR6.
Received September 18, 1989

Abstract: Molecular orbital calculations suggest that an interaction between the substrate amide nitrogen of substituted *N*-benzoylglycine (dithioacyl) papains and the thiol sulfur of cysteine-25 is not only catalytically important, it is part of the catalytic mechanism. AM1 indicates that, during hydrolysis of the dithio ester intermediate, charge is exchanged via orbital interactions and in particular between the HOMOs associated with the reaction site and the LUMOs associated with the benzamide portion of the substrate. Charge delocalization emanating from this effect stabilizes the anionic tetrahedral intermediate formed during deacylation, thereby lowering its activation energy and providing the catalytic effect. The unexpected strong effect of electron-withdrawing and -donating groups (located on the substrate's benzamide phenyl) on deacylation kinetics is explained in terms of their ability to promote or inhibit this charge delocalization. The present computational results together with previous spectroscopic studies suggest that the enzyme specifically promotes this interaction in its binding of the substrate. The relative reactivities of dithio esters and thiol esters are contrasted in terms of their electronic features. Both AM1 and ab initio results indicate a reversal of bond polarity for the C=S bond in the dithio ester moiety [C(=S)—S] relative to the C=O bond in the thiol ester moiety [C(=O)—S]. The approximately 20-fold higher rate of deacylation for the thiol ester relative to the dithio ester may in part be accounted for by the increased stability of the tetrahedral intermediate for the dithio ester relative to the thiol ester.

Introduction

The cysteine proteases comprise a group of proteolytic enzymes which depend on the reactive thiol group (-SH) of a cysteine residue (Cys-25 in papain) for their enzymatic activity. Like the analogous serine proteases, they serve a variety of biological functions although the precise role of many of them remains unknown. The cysteine proteases are widely distributed in nature, including the cathepsins B, H, and L in mammalian tissues, the plant enzymes papain, ficin, bromelain, and actinidin, and the bacterial cysteine proteases clostripain (from *Clostridium histolyticum*) and streptococcal proteinase (from hemolytic streptococci).[1-4]

The crystal structure of papain has been determined at high resolution by X-ray crystallography.[2] Likewise, its binding-site region and proposed mechanism of action have been characterized on the basis of the observed binding of substrate analogues.[2,3] The enzyme is described as being composed of two domains separated by a cleft which contains the active site (Figure 1).[1-4] The binding site for the substrate straddles this cleft with Cys-25 and His-159 located in close proximity but on opposite sides of the cleft. By virtue of its well-positioned imidazole ring [Im], His-159 is believed to act as a general-base catalyst. This might be achieved by forming an ion pair [RS^-·HIm^+] with the thiol group of Cys-25, thereby activating the latter's nucleophilicity.

The reaction pathway for the papain-catalyzed hydrolysis of substrates (Figure 2) can be represented simply as binding, after which the enzyme is first acylated (Figure 2, steps b–d) then deacylated (Figure 2, steps e–f). The overall kinetics of acylation and deacylation is quantified in terms of the specific rate constants k_2 and k_3, respectively. The rate-determining step at both acylation and deacylation is purported to involve formation and subsequent breakdown of a transient anionic tetrahedral intermediate.

The focus of the present study is the catalytic mechanism of the deacylation reaction in papain as a representative cysteine protease. The acylation step, which immediately precedes deacylation, is responsible for the cleavage of peptide bonds in protein substrates. This cleavage yields an intermediate in which the acyl terminal portion of the cleaved substrate forms a bond with the sulfur atom of Cys-25. The intermediate so formed is a thiol ester [C- (=O)—S] in the biological system. As with many other proteases, papain also cleaves ester substrates. Once again, the intermediate formed contains a thiol ester linkage. However, if a thiono ester [C(=S)—O] substrate is used instead of an ester [C(=O)—O] substrate, the resulting linkage is a dithio ester [C(=S)—S]. A minimal reaction scheme for these two possibilities is illustrated in Figure 3.

Certainly, the dithio ester linkage is not indigenous to the biochemistry of cysteine proteases. Yet its unique structural

* Author to whom inquiries should be addressed.
† University of Missouri—St. Louis.
‡ National Research Council of Canada.
‖ Present address: Department of Chemistry, University of Southern California, Los Angeles, CA 90089.

(1) Polgar, L.; Halasz, P. *Biochem. J.* **1982**, *207*, 1. Willenbrock, F.; Kowlessur, D.; O'Driscoll, M.; Patel, G.; Quenby, S.; Templeton, W.; Thomas, E. W.; Willenbrock, F. *Biochem. J.* **1987**, *244*, 173. Asboth, B.; Polgar, L. *Biochemistry* **1983**, *22*, 117. Polgar, L.; Asboth, B. *Proc. FEBS Congr., 16th* (Moscow, June 1984) **1985**, *A*, 17. Willenbrock, F.; Brocklehurst, K. *Biochem. J.* **1985**, *227*, 521.
(2) Kamphuis, G.; Kalk, K. H.; Swarte, B. A.; Drenth, J. *J. Mol. Biol.* **1984**, *179*, 233.
(3) Drenth, J.; Kalk, K. H.; Swen, H. M. *Biochemistry* **1976**, *15*, 3731.
(4) (a) Lowe, G. *Tetrahedron* **1976**, *32*, 291. (b) Fersht, A. *Enzyme Structure and Function*, 2nd ed.; W. H. Freeman and Co.: New York, 1985; p 415.

0002-7863/92/1514-5784$03.00/0

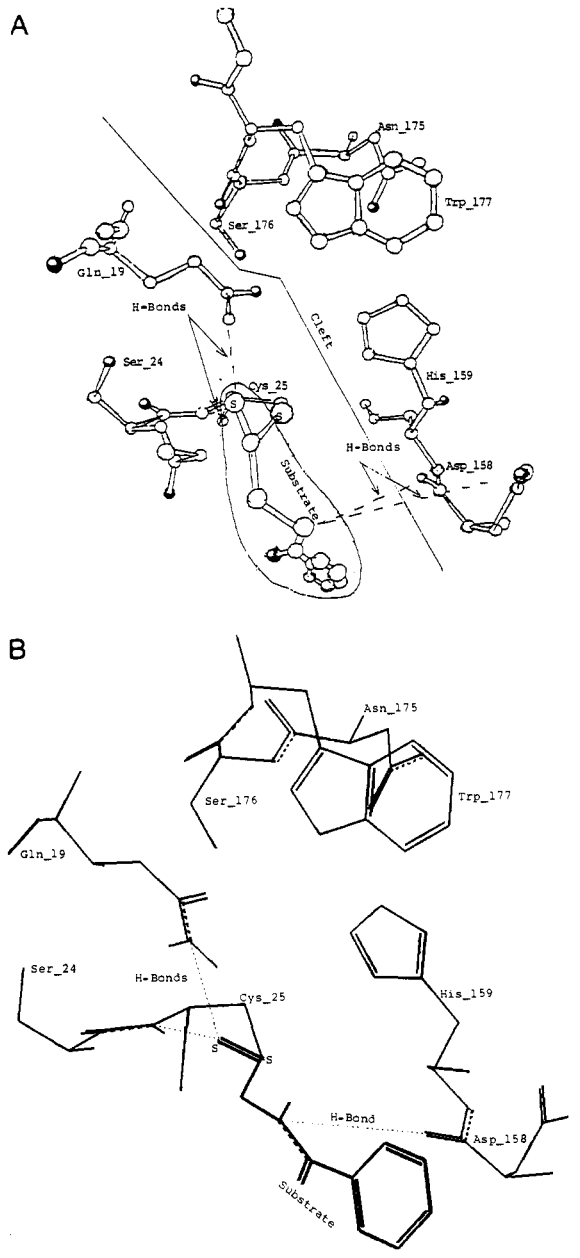

Figure 1. Illustration of the binding-site region of papain taken from the X-ray crystallographic structure (A).[2,3] A sketch of a dithio ester reaction intermediate is inserted to indicate its disposition and the likely binding interactions between the enzyme and bound substrate (B). Hydrogen bonds are indicated as dotted lines.

"footprint" in these systems has been exploited to help elucidate the catalytic mechanism. Such "molecular tagging" of enzymatic reactions is often crucial in experimental investigations, which are hampered by the sheer size and complexity of the enzyme itself and by the variety of distinctive chromophoric groups whose presence often confounds analysis of the catalytic mechanism. With that purpose in mind, Carey et al.[5-11] have taken the resonance Raman spectrum of papain as it reacted with thiono ester [C(=S)—O] substrates leading to the formation of the corresponding dithio ester [C(=S)—S] intermediate.

The practical advantage for Carey et al.[5-11] in introducing the dithio ester linkage was to provide a unique signature in the Raman spectra that was distinct from resonances due to other parts of the enzyme. These Raman spectra were also quite sensitive to conformational and structural changes. By comparing these spectra with those of small, stable, dithio ester model compounds, Carey et al.[5-11] were able to infer analogies between the conformations of the reaction intermediates and those of the model compounds. Concurrent determination of the crystal structures of these model compounds by X-ray crystallographic methods made it possible to deduce the conformation of the reaction intermediate.[6,9,10] At the same time, the crystal structures of the analogous thiol esters were determined.[8] The close parallel between the structures of the thiol esters and corresponding dithio esters provided justification for accepting the results for the dithio esters as pertinent to the biological (viz., thiol ester) system.[8]

One series of substrate–intermediate model compounds that has attracted considerable attention is the *N*-benzoylglycine ethyl dithio esters (Figure 4) with the following ring substitutions (listed in order of increasing electron-withdrawing ability): *p*-OCH_3, *p*-CH_3, *p*-H (i.e., no substituents), *p*-Cl, and *p*-NO_2.[7,11] Their significance stems from the fact that the deacylation rate constants k_3 for the reaction of the corresponding thiono ester [C(=S)—O] substrates with papain showed a strong linear correlation (correlation coefficient $R = 0.99$) with the Hammett σ constant of the substituents. (The empirically-derived Hammett σ constants provide a measure of the electron-donating or -withdrawing ability of a substituent on a benzene ring.[12]) More precisely, the rate of deacylation increased as the electron-withdrawing ability of the substituent increased (as indicated by a more positive Hammett σ).

The unique feature about this effect is that the donating or withdrawing groups are so remote from the reaction site (Figure 5). Furthermore, they are not conjugated to the reaction center in the conventional sense. Other workers[7,11] have attributed this correlation to the variation in a structural parameter identified in the crystal structures, namely, a close (~2.9 Å) nonbonded interaction between the substrate's amide nitrogen and Cys-25's thiol sulfur (Figure 5). These workers have argued that strong electron-withdrawing groups will reduce the amide nitrogen's basicity and hence the strength of the N···S interaction. Postulating this N···S interaction to be rate-limiting, they deduced that strong electron-withdrawing groups on the ring would weaken this presumably rate-limiting N···S interaction and, in so doing, facilitate its breakage and accelerate kinetics.

Our present theoretical analysis, supported by a substantial body of structural data,[6,8,10] disputes the aforementioned explanation in certain key ways. Stated briefly, we found *no correlation* between k_3 and the N···S interaction distances (from either calculated or crystallographic data) among this series of model compounds. In fact, the N···S distance remains virtually constant across this series of model compounds. If this N···S interaction were rate-limiting as proposed by others,[7,11] then k_3 should decrease as the N···S interaction distance decreases (i.e., as this interaction becomes stronger). This lack of correlation is crucial insofar as it suggests an alternative role for the N···S interaction in the catalytic mechanism.

In the present study, we report detailed calculations which suggest that this N···S interaction plays a distinct role in deacylation. On the basis of our theoretical results, as well as corroborating structural evidence, we propose the following alternative mechanism. During the course of attack of the base-assisted nucleophilic water molecule on the acylated enzyme, a negative charge builds up on the reaction center in general and on the thiono

(5) Carey, P. R.; Storer, A. C. *Acc. Chem. Res.* **1983**, *16*, 455.
(6) Varughese, K. I.; Storer, A. C.; Carey, P. R. *J. Am. Chem. Soc.* **1984**, *106*, 8252.
(7) Carey, P. R.; Lee, H.; Ozaki, Y.; Storer, A. C. *J. Am. Chem. Soc.* **1984**, *106*, 8258.
(8) Huber, C. P.; Carey, P. R.; Hsi, S.; Lee, H.; Storer, A. C. *J. Am. Chem. Soc.* **1984**, *106*, 8263.
(9) Angus, R. H.; Carey, P. R.; Lee, H.; Storer, A. C.; Varughese, K. I. *Can. J. Chem.* **1985**, *63*, 2169. Varughese, K. I.; Angus, R. H.; Carey, P. R.; Lee, H.; Storer, A. C. *Ibid.* **1985**, *64*, 1668.
(10) Huber, C. P.; Ozaki, Y.; Pliura, D. H.; Storer, A. C.; Carey, P. R. *Biochemistry* **1982**, *21*, 3109.
(11) Lee, H.; Angus, R. H.; Storer, A. C.; Carey, P. R. *J. Mol. Struct.* **1989**, *214*, 1.
(12) Hammett, L. P. *Physical Organic Chemistry*; 2nd ed.; McGraw-Hill: New York, 1970; p 1.

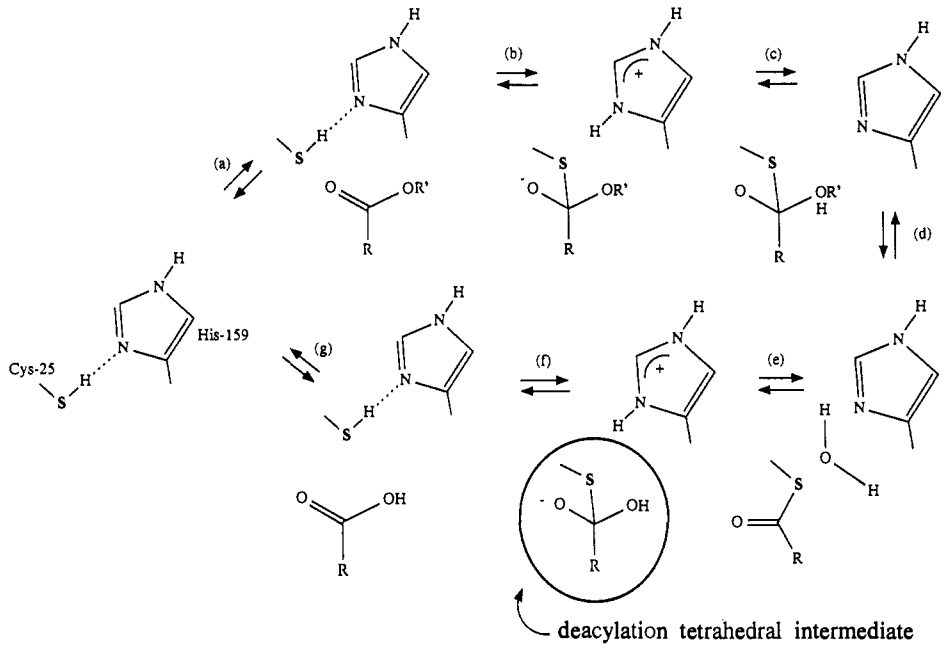

Figure 2. Proposed mechanism of action of papain for the hydrolysis of an ester [RC(=O)—OR'] linkage.[4] The tetrahedral intermediate for the deacylation step is circled.

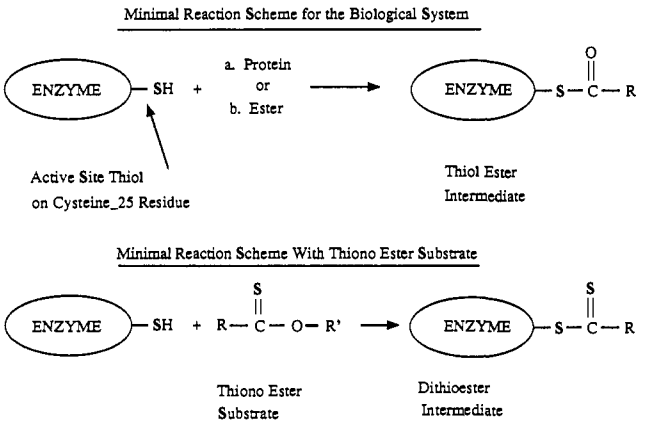

Figure 3. Minimal reaction scheme for the acylation step for the biological system (top) and for the case of a thiono ester substrate as considered in the present study (bottom).

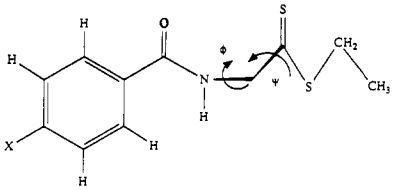

"X" = p-OCH_3, p-CH_3, p-H, p-Cl, p-NO_2

Figure 4. Illustration of the series of dithio ester intermediate model compounds under study. The enzyme portion of the intermediate is represented by the terminal ethyl group.

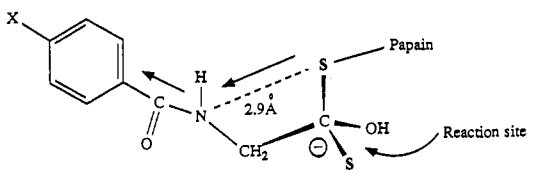

Figure 5. Illustration of the purported anionic tetrahedral intermediate formed by the subject substrates during the deacylation step, with proposed direction for electron delocalization indicated by arrows. Note the remote location of the electron-donating or -withdrawing substituent (denoted by the "X") relative to the reaction site.

sulfur [C(=S)—S] in particular. Meanwhile, the N···S (thiol) interaction serves as a conduit through which electron density in the HOMOs (*h*ighest *o*ccupied *m*olecular *o*rbitals) associated with the reaction site is dispersed into the LUMOs (*l*owest *u*noccupied *m*olecular *o*rbitals) of the benzamide ring system. This charge delocalization process is illustrated in Figure 5. The subsequent dispersal of charge stabilizes the transition state for deacylation, thereby lowering the activation energy and accelerating the kinetics. This charge delocalization will be facilitated by ring substituents which possess strong electron-withdrawing ability (i.e., a more positive Hammett σ).

Our theoretical results support this mechanism by showing strong correlations between k_3 and several calculated parameters which reflect the ring substituent's ability to assist in this delocalization. Furthermore, we present credible evidence suggesting that the charge delocalization mechanism is mediated by a specified HOMO–LUMO interaction. Our proposed mechanism is rendered more persuasive by its consistency with the collection of structural, spectroscopic, and kinetic data pertaining to this series of substrates for papain.

Computational Methodology

The AMPAC program version 2.1[13] provided the AM1,[14] MNDO,[15] and MINDO/3[16] procedures for the present calculations. As the latest and most refined of these procedures, AM1 was employed as the preferred computational tool with MNDO and MINDO/3 included primarily for purposes of comparison. Precedents exist for the use of semiempirical molecular orbital methods in studies of weak intermolecular and charge-transfer interactions, and the results obtained compare favorably with those obtained by ab initio methods.[17] AM1 was developed in part as an improved version of MNDO and treats hydrogen bonding more realistically than its predecessor.[13,14,18] This fact made its use

(13) Liotard, D. A.; Healy, E. F.; Ruiz, J. M.; Dewar, M. J. S. AMPAC, Version 2.1; QCPE Program No. 506, Quantum Chemistry Program Exchange, Indiana University, Bloomington, IN. AMPAC 2.1 includes explicit AM1 parameters for all atom types found in the subject molecules including the sulfur atom type. The source of these "sulfur" parameters is as follows: Dewar, M. J. S.; Yuan, Y.-C. *Inorg. Chem.* **1990**, *29*, 3881.

(14) Dewar, M. J. S.; Zoebish, E. G.; Healy, E. F.; Stewart, J. J. P. *J. Am. Chem. Soc.* **1985**, *107*, 3902.

(15) Dewar, M. J. S.; Thiel, W. *J. Am. Chem. Soc.* **1977**, *99*, 4899.

(16) Part XXVI: Bingham, R. C.; Dewar, M. J. S.; Lo, D. H. *J. Am. Chem. Soc.* **1975**, *97*.

(17) Glauser, W. A.; Raber, D. J.; Stevens, B. *J. Comput. Chem.* **1988**, *9*, 539.

Table I. Comparison of Selected Structural and Electronic Parameters for the Parent Compound *N*-Benzoylglycine Ethyl Dithio Ester, as Derived from the Crystal Structure[6] and the Present Calculations

	torsion angles[a]		interaction distances and bond lengths[b]			atomic partial charges for [C(=S)—S] linkage[c]		
method	ϕ	ψ	N···S	C—S	C=S	C	=S	—S
X-ray[d]	−78.7	−15.5	2.866	1.710	1.615			
MINDO/3[e]	−88.8	−11.6	2.758	1.732	1.595	0.448	−0.375	−0.265
MNDO[e]	−83.2	−19.1	2.868	1.681	1.560	−0.283	0.002	0.139
AM1[e]	−107.3	−46.9	3.025	1.680	1.545	−0.359	0.049	0.189

[a] In units of degrees. [b] In units of angstroms. [c] In units of fraction of a unit charge. [d] Reference 6. [e] Present work.

especially appropriate for modeling the biological reaction mechanisms considered herein.

In all AM1 computations, the default BFGS[19] method was implemented for geometry optimization via energy minimization. The PRECISE option was exercised, as recommended,[18] to augment the stringency of the convergence criteria for both the self-consistent-field (SCF) and geometry-optimization iterations.

The conformation of a given model compound is described in terms of the torsion angles ϕ and ψ (Figure 4), by analogy to the familiar Ramachandran angles ϕ and ψ defined for the torsions around backbone bonds in proteins. Values of the conformational energy ΔE were determined by taking differences between the heats of formation ΔH_f calculated by AM1 for those conformations. Relative differences in energy between molecules before and after the attack by the hydroxyl nucleophile were also determined in this way. This technique was used, in particular, to determine the relative stability of the molecules for different values of the torsion angle ψ. This angle is especially pertinent in the present context since it dictates the symmetry and proximity of the forementioned interaction between the amide nitrogen and each of the two sulfur atoms [C(=S)—S]. These separate but related N···S interactions punctuate the difference between the two conformations designated "A" and "B" (vide infra).

Ab initio calculations were carried out using the GAUSSIAN 82 program[20] using both 3-21G* and 6-31G* basis sets. For the sake of computational efficiency, these calculations were confined to small model compounds such as $CH_3C(=S)SCH_3$ and $CH_3C(=O)SCH_3$. The purpose here was to compare the resulting charge distributions and bond moments with the corresponding values derived from AM1 calculations.

The initial structural geometry for each dithio ester model compound under study was taken from the published crystal structure of the parent ("X" = H in Figure 4) *N*-benzoylglycine ethyl dithio ester followed by AM1 optimization.[6] Molecular computer graphics display, manipulation, and analysis of input and output molecular structures were achieved using the molecular modeling programs Chem-X and Insight/Discover.[21]

It is perhaps necessary for us to stress that we do not regard the calculated parameters such as the atomic partial charges or even the heats of formation for molecules as exact or "true". However, within a single computational method, such as AM1, trends can be spotted in calculations on a series of molecules. And among computational methods, such as AM1, MNDO, and ab initio, qualitative agreement on features such as the direction of bond dipoles adds to our confidence in their qualitative correctness.

Results and Discussion

Conformational Features. The model compounds included in our computational investigations are illustrated in Figure 4. All have been shown to crystallize in the B conformation (Figure 6),

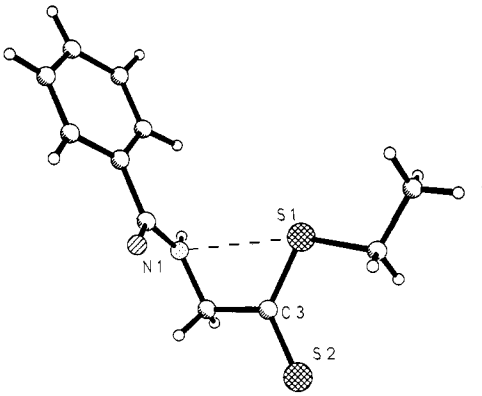

Figure 6. Parent *N*-benzoylglycine ethyl dithio ester shown in the conformation designated "B". The characteristic short N···S(thiol) interaction distance is indicated.

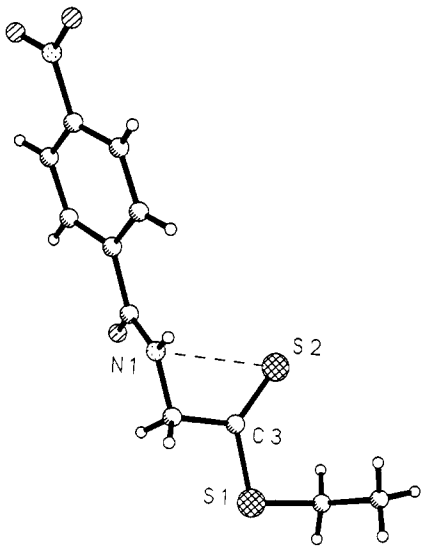

Figure 7. *N*-(*p*-Nitrobenzoyl)glycine ethyl dithio ester shown in the conformation designated "A". The characteristic short N···S(thiono) interaction distance is indicated.

apart from the *p*-nitro compound which crystallizes in the A conformation (Figure 7). In addition, the resonance Raman data indicated that the enzyme–substrate intermediates modeled by these molecules exclusively adopted the B conformation in the active site.[5-11]

The characteristic structural features of these conformations were quite consistent among the different compounds. Most notably, conformation B (Figure 6) featured a strong nonbonded interaction between the amide nitrogen and the thiol sulfur [—S—], and their approach distance (ca. 2.9 Å) was less than the sum of their van der Waals radii by ~0.35 Å. In the A conformation (Figure 7), the amide nitrogen appeared to interact similarly with the thiono sulfur [=S].

The values of several important structural parameters for these model compounds, as obtained by the present calculations and from the crystal structures, are summarized in Table I. These results show that, starting with *N*-benzoylglycine ethyl dithio ester

(18) Boyd, D. B.; Smith, D. W.; Stewart, J. J. P.; Wimmer, E. *J. Comput. Chem.* **1988**, *9*, 387.

(19) BFGS (Broyden–Fletcher–Goldfarb–Shanno) method: (a) Broyden, C. G. J. *Inst. Math. Appl.* **1970**, *6*, 222. (b) Fletcher, R. *Comput. J.* **1970**, *13*, 317. (c) Goldfarb, D. *Mathematics of Computation* **1970**, *24*, 23. (d) Shanno, D. *J. Optim. Theory Appl.* **1985**, *46*, No. 1, 87.

(20) Binkley, J. S.; Frisch, M. J.; DeFrees, D. J.; Krishnan, R.; Whiteside, R. A.; Schlegel, H. B.; Fluder, E. M.; Pople, J. A. *Gaussian 82*; Carnegie-Mellon Chemistry Publishing Unit: Pittsburgh, PA, 1982.

(21) Chem-X, a product of Chemical Design, Ltd., Oxford, UK. Insight and Discover, products of Biosym Technologies, Inc., San Diego.

Table II. Comparison of Selected Structural and Electronic Parameters for Dimethyl Dithio Ester and Dimethyl Thiol Ester Model Compounds, as Derived from the Present Semiempirical and ab Initio Molecular Orbital Calculations

	bond lengths[a]		bond angles[b]		atomic partial charges on [C(=X)—S)][c]		
	C=X	C—S	θ	θ'	C	X	S
Dimethyl Dithio Ester (X = S)							
MINDO/3	1.594	1.730	104.0	119.2	0.480	−0.379	−0.244
MNDO	1.557	1.728	110.5	111.1	−0.261	−0.005	0.131
AM1	1.547	1.683	111.0	107.0	−0.345	−0.018	0.210
HF/3-21G*	1.621	1.740	111.1	103.8	−0.333	−0.068	0.315
HF/6-31G*	1.625	1.744	111.1	104.4	−0.188	−0.158	0.237
Dimethyl Thiol Ester (X = O)							
MINDO/3	1.191	1.756	102.7	124.1	0.722	−0.491	−0.357
MNDO	1.224	1.713	113.1	111.8	0.138	−0.289	0.305
AM1	1.235	1.708	113.9	104.9	0.100	−0.298	0.115
HF/6-31G*	1.187	1.784	114.0	99.8	0.451	−0.504	0.110

[a] In units of angstroms. [b] θ = ⟨C–C(X)–S and θ' = ⟨C(X)–S–C, in units of degrees. [c] In units of fraction of a unit charge.

in a B-type conformation, each of the semiempirical molecular orbital methods finds a local energy minimum reasonably nearby. It may seem disconcerting to find that these calculated conformations (i.e., ϕ and ψ) do not agree precisely with the corresponding values derived from the X-ray crystallographic data. However, some discrepancy is expected in that the structural and conformational parameters of a compound in its crystalline environment (i.e., interacting with other molecules) will differ at least somewhat from those obtained for the isolated molecule, as depicted by the theoretical approaches employed in the present study. It is therefore quite acceptable that these calculations find a local minimum energy conformation for the model compound reasonably near the B conformation.

Electronic Features. Another, more intriguing feature of the computational results also appears in Table I. First, both AM1 and MNDO predict that the C=S and C—S bonds of the [C(=S)—S] moiety will have bond dipoles with the negative pole pointing toward the carbon and the positive pole pointing toward the sulfur. As a consequence, a highly negative charge density is centered on the carbon. This result would imply that the carbon atom in the [C(=S)—S] linkage provides a *poor site* for nucleophilic attack. This peculiarity of the dithio ester [C(=S)—S] intermediate was highly unexpected given what one would expect for a system chosen specifically[7,11] to model the thiol ester [C(=O)—S] intermediate found in the biological system. Indeed, subsequent calculations on the corresponding thiol ester yielded precisely the opposite case, i.e., an electron-poor carbon, a *good site* for nucleophilic attack.

To corroborate the results of these AM1 calculations, we carried out a series of calculations on a dimethyl dithio ester [$CH_3C(=S)SCH_3$] and a dimethyl thiol ester [$CH_3C(=O)—SCH_3$] using both semiempirical and ab initio methods. Some differences in the magnitudes of the charge distributions are apparent between the ab initio and semiempirical methods. At the same time, Table II shows that the ab initio calculations substantiate the AM1 results for the dithio ester in terms of the enhanced electron population around the carbon and the directional sense of the bond dipoles.

A survey of the literature provides corroborative support for this view of the "reverse" polarity (i.e., C←S) of the C=S bond,[22] especially concerning the regiochemistry of addition of organometallic sources of carbanion (e.g., Grignard and organolithium reagents).[23-25] Furthermore, published values of the electronegativities of carbon, oxygen, and sulfur indicate only slight differences in electronegativity between sp^3 carbon and sp^3 sulfur.[26]

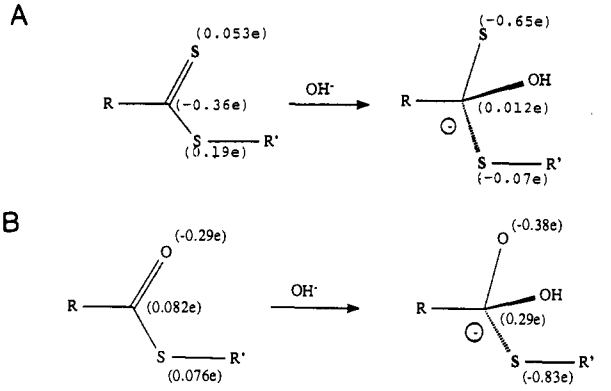

Figure 8. Illustration of the tetrahedral intermediate formed by hydroxyl attack on the dithio ester (A) and on the thiol ester (B). Some pertinent values of the AM1-calculated atomic partial charges are indicated for the case R = $PhC(O)NHCH_2$ and R′ = Et.

This appears to leave the polarity of the C=S bond open to question. Finally, the ab initio calculations of Fausto et al.[27] yielded charge distributions very similar to ours for a related set of dithio esters and dithio acids.

The charge distribution around the reactive site is not a trivial point. The deacylation reaction is postulated to proceed via a general-base-catalyzed step in which either an imidazole ring from the nearby His-159 or, less likely, a carboxylate anion from the somewhat more distant Asp-158 (Figure 1) is thought to donate electron density to the water nucleophile attacking at the carbonyl carbon adjacent to the scissile bond. (Figure 2 illustrates this process for the case of His-159 serving as the general base.) This donation allows the reaction to proceed without building a strong positive charge on the water molecule.[4,28,29] Inasmuch as the carbonyl carbon serves to accept the electron-rich nucleophile, it is evident that the magnitudes and orientations of the dipoles are critical to the mechanism and kinetics of the reaction.[30] In an attempt to reconcile this apparent paradox, we posed the following question: "*How then might the deacylation of (dithioacyl)papain [C(=S)—S-papain] occur by the same mechanism as the deacylation of acylpapain [C(=O)—S-papain]?*"

We sought an answer in the high polarizability of the sulfur atom, since this feature would render the electron density around the sulfur atom more sensitive to its local environment. We ran several AM1 calculations in which the model dithio esters were placed in the context of their environment within the active site. Variations upon this theme which were attempted included calculations with carboxylate anions in close proximity to the thiono sulfur, carboxylate anions in close proximity to the thiol sulfur, and water molecules hydrogen-bonded to the amide nitrogen. The results from these preliminary calculations foretold that the charge distribution around the dithio ester could be altered significantly. None, however, produced results so dramatic as those obtained

(22) Lumbrusco, H.; Andrieu, C. *Bull. Soc. Chim. Fr.* **1966**, No. 10, 3201.
(23) Beak, P.; Worley, J. W. *J. Am. Chem. Soc.* **1970**, *92*, 4142.
(24) Leger, L.; Saquet, M. *Bull. Soc. Chim. Fr.* **1975**, Nos. 3-4, 657.
(25) Bertz, S. H.; Dabbagh, G.; Williams, L. M. *J. Org. Chem.* **1985**, *50*, 4414.

(26) The electronegativities for the C, O, and S atoms are as follows:

	C	O	S
Pauling[a]	2.55	3.44	2.58
Allred-Rochow[b]	2.50	3.50	2.44
Mulliken[c]	2.63	3.17	2.41

(a) Pauling, L. *The Nature of the Chemical Bond*, 3rd ed.; Cornell Univ. Press: Ithaca, NY, 1960; p 93. (b) Allred, A. L. *J. Inorg. Nucl. Chem.* **1961**, *17*, 215. Allred, A. L.; Rochow, E. G. *Ibid.* **1958**, *5*, 264 and 269. (c) Mulliken, R. S. *J. Chem. Phys.* **1934**, *2*, 782. Mulliken, R. S. *Ibid.* **1935**, *3*, 573.

(27) Fausto, R.; Teixeira-Dias, J. J. C.; Carey, P. R. *J. Mol. Struct. (Theochem.)* **1987**, *152*, 119. Fausto, R.; De Carvalho, L. A. E. Batista; Teixeira-Dias, J. J. C. *J. Mol. Struct. Theochem.*) **1990**, *207*, 67. Teixeira-Dias, J. J. C.; Fausto, R.; De Carvalho, L. A. E. Batista *J. Comput. Chem.* **1991**, *12*, 1047.
(28) Zannis, V. I.; Kirsch, J. F. *Biochemistry* **1978**, *17*, 2669.
(29) Rullman, J. A. C.; Bellido, M. N.; van Duijnen, P. T. *J. Mol. Biol.* **1989**, *206*, 101.
(30) Bürgi, H. B.; Dunitz, J. D.; Lehn, J. M.; Wipff, G. *Tetrahedron* **1974**, *30*, 1563.

when we attempted to model the attack of the nucleophile and subsequent formation of the tetrahedral intermediate in the deacylation step.

Modeling the Attack of the Nucleophile. This series of calculations was aimed at simulating the formation of the anionic tetrahedral intermediate in the deacylation step. For each model compound, AM1 calculations were run on the anion formed by "attaching" an OH^- to the carbon atom of the dithio ester [C(=S)—S] moiety. The results were intriguing. Starting with the dithio ester moiety in a nearly coplanar geometry, AM1 optimized it to a tetrahedral configuration (Figure 8) as expected for the anionic reaction intermediate during deacylation. After attack, both the C—S and C=S bonds elongated by ~0.14 Å, a noteworthy result in view of the fact that formation of this intermediate was the prelude to the breaking of the former bond.

Of potentially greater significance (in light of our previous concerns) was the way in which the charge distribution was altered by the attack itself. This is illustrated in Figure 8 for the case of both the dithio ester [C(=S)—S] and thiol ester [C(=O)—S]. Upon approach of the OH^- nucleophile to the dithio ester, AM1 indicates that the bond dipoles repolarize to render an attack on the carbon atom more favorable. In terms of the atomic partial charges, the C, S(thiono), and S(thiol) change, respectively, from $-0.36e^-$, $0.053e^-$, and $0.19e^-$ *before* attack to $0.012e^-$, $-0.65e^-$, and $-0.07e^-$ *after* attack (see Figure 8).

Similar "before attack vs after attack" AM1 calculations were run on the corresponding thiol ester, as found in the biological system. These produced two striking and related differences. First, for the anionic tetrahedral intermediate formed in this case, the partial charge on the thiol sulfur [-S-] is much more negative ($-0.83e^-$). Second, the scissile C—S(thiol) bond is elongated to the verge of severance, from 1.73 to 3.83 Å, while the C=O bond is elongated only slightly from 1.23 to 1.25 Å. Furthermore, the partial charge on the carbonyl oxygen changes only slightly during the attack, from -0.29 to $-0.38e^-$.

In light of the preceding considerations, the following qualitative picture is emerging regarding the electronic features of the deacylation reaction. We may deduce that, in the attack by the hydroxyl nucleophile on the dithio ester [C(=S)—S], much of the increased electron density is donated into the low-lying π^* antibonding orbitals of the C=S bond. However, for the thiol ester [C(=O)—S] case, the σ^* antibonding orbitals of the C—S bond lie relatively lower in energy compared with π^* antibonding orbitals of the C=O bond. We conclude that, for the thiol ester case, the σ^* antibonding orbitals of the C-S bond accept proportionally more of the increased electron density of the reactive center. Consistent with our calculations, this would yield a scissile C-S bond which is even weaker and correspondingly longer. Furthermore, it implies that the intermediate in the deacylation of the thiol ester (i.e., the biological system) is closer to severance of the scissile C-S bond and thus farther along the reaction coordinate toward formation of products.

Of more general significance, in both examples cited above the sulfur atom acts as an "electron sink" by absorbing the additional electron density and thereby stabilizing the anionic tetrahedral intermediate. This would suggest a greater stability for the intermediate in the deacylation of the dithio ester (by virtue of its double complement of sulfur atoms). At the same time, it offers an explanation for the approximately 20-fold higher rate of deacylation for the thiol ester as opposed to the dithio ester.[5]

We can now propose how the hydrolysis of the dithio ester could proceed via a mechanism similar to that for the thiol ester. Specifically, the approach of the nucleophile alters the electronic distribution around the [C(=S)—S] reactive center. This in turn changes the bond dipoles to make the carbon atom more receptive to the attack by the nucleophile. In addition, the heat of formation data indicate that the intermediate in the deacylation of the dithio ester [C(=S)—S] is further stabilized by the presence of the thiono sulfur which of course is absent in the thiol ester [C(=O)—S].

A Conformer vs the B Conformer: Implications for Binding and Electronic Structure. Additional calculations were performed to compare the relative stabilities of the A and B conformers for the dithio ester model compounds. The characteristic difference between these two conformers can be described principally by the torsion angle ψ (Figure 4). Starting with optimized geometries for the B conformers of the *p*-methoxy and the *p*-nitro model compounds of our series, we ran calculations freezing this torsion angle at specified intervals around the bond. After this torsion angle was frozen, the remainder of the molecule was allowed to relax to a local minimum energy conformation.

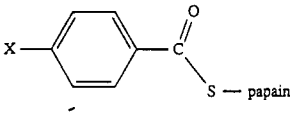

X = OCH_3, CH_3, H, Cl, NO_2

Figure 9. Illustration of the series of benzoyl–papain intermediates studied by Zannis and Kirsch.[28]

The results of these calculations confirm that local energy minima exist near both the A conformation and the B conformation. However, the heat of formation data indicate that the A conformation is favored energetically over the B conformation by ~1.2 kcal/mol for both the *p*-nitro compound and the *p*-methoxy compound. This result must be interpreted in light of the resonance Raman evidence obtained for the dithioacyl–enzyme intermediates which indicates that the B conformer is adopted exclusively in the active site. On the other hand, FTIR studies[7,8] indicate that in solution the model compounds have an equilibrium distribution of A and B conformers as well as a third conformer designated C5. The C5 conformer has not been observed in any of the crystal structures, but its existence has been inferred from the spectroscopic data. The relative populations show a dependence upon the hydrogen-bonding ability and polarity of the solvent.

While the present computational studies do not account for solvent effects, none of the solvent systems studied experimentally[7,8] hint that they force the exclusive adoption of the B conformation. This observation supports our suggestion that the binding of the substrates in the active site changes the relative energies of the separate conformers to favor conformer B. This change is apparently such that only the B conformation is detectable in the active site using resonance Raman spectroscopic methods.

Some sense of the overall morphology of the enzyme is helpful in developing an understanding of the role binding plays in defining substrate conformation. The enzyme has been described as being composed of two domains with a cleft between them which contains the active site (Figure 1).[1-4] Fersht[4b] describes evidence for a binding pocket for the substrate's carbonyl oxygen of the carbon attached to Cys-25 located on the same side of the cleft as Cys-25 and comprised of the backbone NH group of Cys-25 and the side chain NH_2 of Gln-19. Lowe[4a] indicates that model-building evidence supports the existence of a hydrogen bond between the substrate's amide nitrogen and the backbone carbonyl of aspartate-158 positioned on the opposite side of the cleft, and Drenth et al.[3] offer crystallographic evidence that this interaction is bridged by a water molecule. Insofar as the substrate's thiono sulfur is pinned in this way to one side of the cleft and its amide nitrogen is hydrogen-bonded to the opposite side (see Figure 1), it would appear that these tetherlike interactions would favor the B conformer over the alternative A conformer. By the same token, this view of the substrate as being tethered in the active site would help explain the enzyme's stereoisomeric and conformational specificity.[5-11]

Structural and Electronic Effects on Deacylation Kinetics. Zannis and Kirsch[28] earlier discovered a correlation between the rate of deacylation for substituted benzoyl papains (Figure 9) and the Hammett σ for the corresponding substituent. They found that benzoyl papains substituted with electron-withdrawing groups were observed to deacylate more quickly, while those with electron-donating groups deacylated more slowly. The rate of deacylation again correlated with the strength of the electron donation or withdrawal.

Table III. Comparison of the Deacylation Rate Constant k_3 and Selected AM1-Calculated Structural and Electronic Parameters for the Series of Substituted *N*-Benzoylglycine Ethyl Dithio Ester Compounds under Study

			interaction distances and bond lengths[b]			atomic partial charges on [C(=S)—S][c]		
subst	Hammett σ	k_3[a]	N···S	C=S	C—S	C	S	S
p-OCH_3	−0.28	0.030	3.023	1.545	1.680	−0.3597	0.0519	0.1887
p-CH_3	−0.17	0.061	3.023	1.545	1.680	−0.3600	0.0524	0.1888
p-H	0.00	0.082	3.001	1.545	1.680	−0.3586	0.0491	0.1886
p-Cl	0.23	0.093	3.022	1.545	1.680	−0.3615	0.0562	0.1875
p-NO_2	0.78	0.178	3.019	1.544	1.680	−0.3656	0.0650	0.1852

[a] In units of s^{-1}. Data collected from ref 5–11. [b] In units of angstroms. [c] In units of fraction of a unit charge.

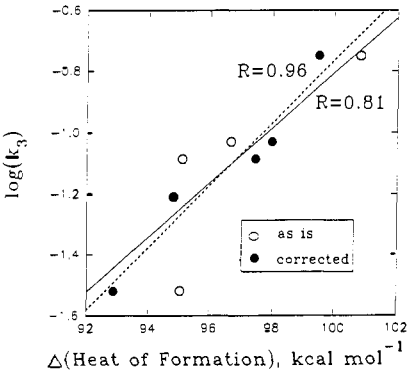

Figure 10. Plot of the AM1-calculated relative heats of formation before and after hydroxyl attack $\Delta(\Delta H_f)$ versus the logarithm of the deacylation rate constant k_3 for the series of *N*-benzoylglycine ethyl dithio ester model compounds under study. The solid line refers to the "as is" data (R = 0.81); the dashed line refers to the "corrected" data (R = 0.96).

More recent investigations into the deacylation of substituted *N*-benzoylglycine dithioacyl papains established a similar correlation between deacylation kinetics and the Hammett σ or basicity of the corresponding benzamide.[5-11] What is unique about the latter case is that this effect has been observed for electron-withdrawing or -donating groups which are very remote from the site of the deacylation (Figure 5). They are likewise not conjugated to the reactive center; consequently, delocalization via a through-bond mechanism is unlikely.

The strong correlation between the k_3 values and the Hammett σ constants of the substituents led Carey et al.[7,11] to conjecture that the basicity of the substrate's amide nitrogen might have an effect on the strength of the N···S thiol interaction. This basicity would be modulated by donor or withdrawing groups on the ring. If, as they proposed,[7,11] breakage of this N···S interaction were rate-limiting, we might expect to see some correlation between the N···S interaction distance and the deacylation rate constant k_3. However, inspection of the spread of values calculated for this interaction distance among the model compounds showed a variation of less than 0.03 Å (Table III). These results hardly seemed significant. When the corresponding deacylation rate constants k_3 were plotted against these values, *no correlation* was observed. Similarly, the crystal structure data revealed a lack of correlation between the N···S distance and k_3.[6,8,9,10,31] Furthermore, our calculations which modeled the attack of a hydroxyl on these model compounds (to simulate the formation of the tetrahedral intermediate) indicated that severance of the N···S thiol interaction was not a prerequisite for the transition state to form. In fact, in one case this interaction distance became slightly smaller in the tetrahedral intermediate.

To investigate this phenomenon further, we returned to our calculations on the series of model compounds illustrated in Figure 4 and their corresponding tetrahedral intermediates. The difference in heat of formation between the neutral molecule and the tetrahedral intermediate, designated $\Delta(\Delta H_f)$, was plotted against the logarithm of k_3 (Figure 10). The degree of correlation (R = 0.81) was encouraging but not compelling. Yet the presence

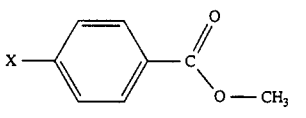

X = OCH_3, CH_3, CH_2CH_3, H, F, Cl, Br, COOH, NO_2

Figure 11. Illustration of the series of X-substituted methyl benzoates utilized for development of "correction factors".

of a slight but persistent curvature in all of our correlation plots suggested to us that other, external factors might be diminishing an otherwise strong correlation. We thus turned to address this matter in greater detail.

Others have attempted to correlate the differences in the acidity of substituted benzoic acids with computationally derived parameters. These differences are widely accepted as being due to the variable ability of the anion to decrease the charge density on the carboxylate oxygens.[12] La Manna et al.[32] have studied this system with ab initio methods, and Sotomatsu et al.[33] have used AM1. Both sets of authors explored the relationship between experimental gas-phase acidities and the calculated difference in ΔH_f for the benzoate anion. They also looked for correlations with the energy of the HOMO of the benzoate anion. Sotomatsu et al.[33] also compared these parameters with the Hammett σ for the substituents.

In both of these investigations,[32,33] a high degree of correlation was found between the gas-phase acidities and the abovementioned parameters (i.e., the $\Delta(\Delta H_f)$ and the energy of the benzoate's HOMO). Sotomatsu et al.[33] noted however that correlation with Hammett's σ was much poorer. This suggested to us that difficulties might arise when the in vacuo calculation results are applied to condensed-phase systems. Nevertheless, we believed that the errors, if due to solvent effects, might be consistent between calculations on similar systems that show these substituent effects. If so, it might be possible to develop suitable correction factors for each substituent. We have already demonstrated the utility of applying such empirically-derived scaling factors in other applications.[34]

These empirical correction factors were derived and implemented in the following manner. We ran AM1 calculations on a reaction that had many similarities with the one we were studying: the base-catalyzed hydrolysis of the series of substituted methyl benzoate esters illustrated in Figure 11. The rate of this reaction also showed strong dependence on the ring's substituent; this particular reaction was in fact used in the formulation of Hammett's original σ parameters.[12] Our calculations again modeled the attack of the hydroxyl nucleophile and the formation of the tetrahedral intermediate. For this series we plotted the AM1-calculated $\Delta(\Delta H_f)$ values against the Hammett σ for each ring substituent. A best-fit line was determined, and for each substituent a scalar correction factor was calculated (Table IV). This factor, when multiplied by $\Delta(\Delta H_f)$ for the substituent, places the point on this best-fit line (Figure 12).

(31) Huber, C. P. Unpublished data.

(32) La Manna, G.; Tschinke, V.; Paolini, L. *J. Chem. Soc., Perkin Trans. 2* **1985**, 1393.

(33) Sotomatsu, T.; Murata, Y.; Fujita, T. *J. Comput. Chem.* **1989**, *10*, 94.

(34) Welsh, W. J.; Yang, Y. *Comput. Polym. Sci.* **1991**, *1*, 139.

Table IV. List of Hammett σ Parameters and AM1-Calculated Values of $\Delta(\Delta H_f)$ for the Series of X-Substituted Methyl Benzoates. Also Included Are Values of the "Corrected" $\Delta(\Delta H_f)$ and the Individual Correction Factors[a]

X-substituent	Hammett σ	$\Delta(\Delta H_f)$[b] "as is"	$\Delta(\Delta H_f)$[b] "corrected"	correction factor[c]
OCH_3	−0.28	77.4775	75.7128	0.9772
CH_3	−0.17	77.2742	77.2502	0.9997
CH_2CH_3	−0.15	77.4089	77.5297	1.0016
H	0.0	77.7018	79.6262	1.0248
F	0.06	81.3049	80.4648	0.9843
Cl	0.23	81.7485	82.8407	1.0134
Br	0.23	82.6236	82.8407	1.0026
COOH	0.45	85.4164	85.9155	1.0058
NO_2	0.78	91.7526	90.5277	0.9867

[a] Least-squares best-fit line corresponds to the following equation: "corrected" $\Delta(\Delta H_f) = \sigma(13.9763) + 79.6262$, for which $R = 0.97$. [b] In units of kcal mol^{-1}. [c] Correction factor = ["corrected" $\Delta(\Delta H_f)$]/["as is" $\Delta(\Delta H_f)$].

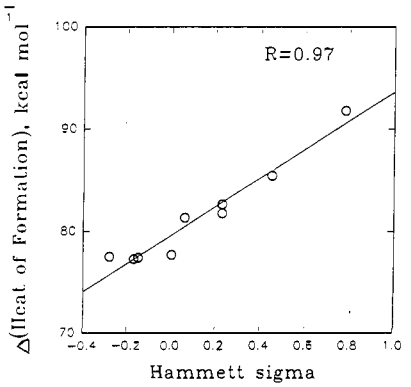

Figure 12. Plot of AM1-calculated $\Delta(\Delta H_f)$ versus the Hammett σ for the series of X-substituted methyl benzoates. The data plotted here is found in Table IV.

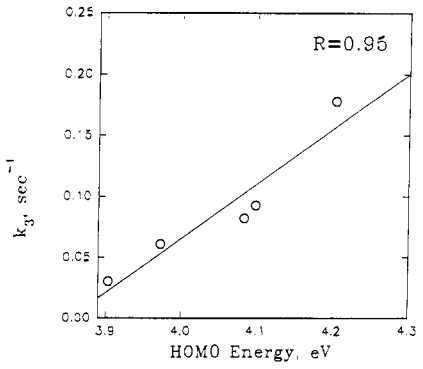

Figure 13. Plot of the "corrected" energy of the HOMO of the tetrahedral intermediate for the model compounds under study versus the deacylation rate constant k_3.

We proceeded to apply these correction factors for each substituent to the $\Delta(\Delta H_f)$ results for our series of *N*-benzoylglycine ethyl dithio ester model compounds (Table V). The correlation coefficient for the $\Delta(\Delta H_f)$ vs log k_3 plot improved dramatically, from $R = 0.81$ to 0.96 (see Figure 10). Assuming $\Delta(\Delta H_f)$ to be proportional to the activation energy for the deacylation, we viewed this result as validation that AM1 discerned a decrease in the activation energy commensurate with an increase in the electron-withdrawing ability of the ring substituent.

We corrected the energies for the HOMOs of the anionic tetrahedral intermediate in a similar way (Table V and VI). In a manner analogous to the approach of La Manna et al.[32] and Sotomatsu et al.,[33] we plotted these values vs k_3 for our series of *N*-benzoylglycine ethyl dithio esters (Figure 13). It is generally understood that the difficulty in removing an electron from the negatively charged intermediate will increase directly as the

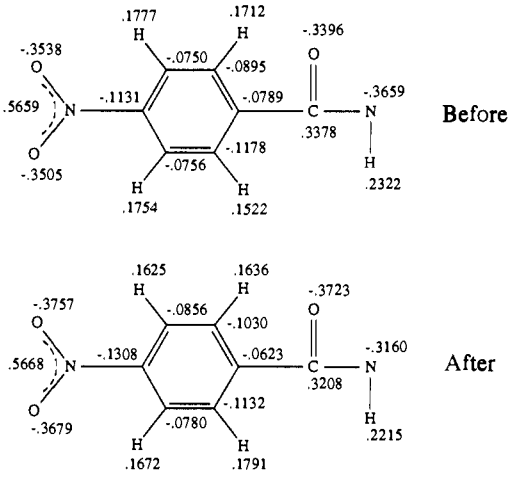

Figure 14. Illustration of the benzamide fragment for the *p*-nitro model compound showing the AM1-calculated partial atomic charges, both before and after OH^- attack.

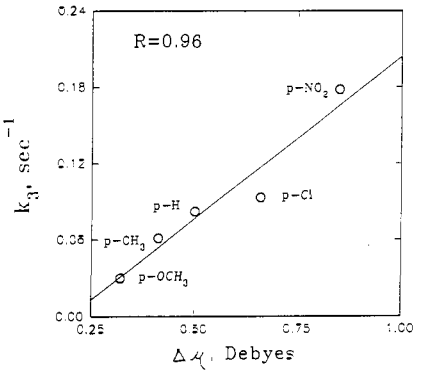

Figure 15. Plot of the change in the calculated dipole moment ($\Delta\mu$) of each molecular fragment before relative to after hydroxyl attack versus the deacylation rate constant k_3.

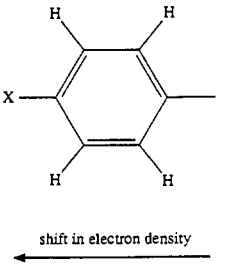

Figure 16. Illustration of the benzyl moiety of the model compounds used for the $\Delta\mu$ calculations. The arrow indicates the shift in electron density toward the ring system, as modulated by the electron-withdrawing ability of the *p*-X substituent.

negative charge becomes more stabilized (via delocalization). The correlation coefficient for this "corrected" plot was 0.95. The consistently high degree of correlation found in these plots suggested to us that strong electron-withdrawing groups might be reducing the activation energy for the deacylation reaction and, if true, that the reason might be due to better delocalization of the anionic tetrahedral intermediate's charge onto the benzamide portion of the substrate.

We made several other plots from our calculations which helped to substantiate this hypothesis. On a qualitative level, we asked whether this charge delocalization extended over the entire benzamide ring system. The answer was in the affirmative, as illustrated in Figure 14 where the AM1-calculated charge distribution (for the case $X = NO_2$) is mapped out both "before" and "after" attack by the OH^- (representing the base-assisted water nucleophile). This finding confirmed that the overall $-1.0e^-$ charge of the anionic tetrahedral intermediate was indeed being partially

Table V. AM1-Calculated Values of $\Delta(\Delta H_f)^a$ and the Energy[b] of the HOMO and the LUMO of the Tetrahedral Intermediate for Our Series of X-Substituted *N*-Benzoylglycine Ethyl Dithio Esters[d]

X-substituent	k_3	Hammett σ	$\Delta(\Delta H_f)^a$ "as is"	$\Delta(\Delta H_f)^a$ "corrected"	HOMO energy[b] "as is"	HOMO energy[b] "corrected"	LUMO energy[b]
OCH_3	0.030	−0.28	95.026	92.860	−3.997	−3.903	2.297
CH_3	0.061	−0.17	94.802	94.774	−3.973	−3.972	2.251
H	0.082	−0.00	95.082	97.440	−3.980	−4.083	2.308
Cl	0.093	0.23	96.672	97.967	−4.054	−4.098	1.929
NO_2	0.178	0.78	100.822	99.481	−4.254	−4.203	0.745
corr coeff R[c]			0.81	0.96	0.92	0.95	

[a] In units of kcal mol^{-1}. [b] In units of eV. [c] Correlation coefficients for least-squares best-fit line, as given in Figures 10 and 13. [d] The $\Delta(\Delta H_f)$ and HOMO energies are given both "as is" and as corrected by coefficients taken from analysis of the hydrolysis of the corresponding methyl benzoates. Also included are the values of k_3 and the Hammett σ constants.

Table VI. List of Hammett σ Parameters and AM1-Calculated Values of the Energy of the HOMO for the Tetrahedral Intermediate for the Series of X-Substituted Methyl Benzoates. Also Included Are the Associated "Corrected" HOMO Energies and Individual Correction Factors[a]

X-substituent	Hammett σ	HOMO energy, "as is"[b]	HOMO energy, "corrected"[b]	correction factor[c]
OCH_3	−0.28	4.499	4.393	0.9765
CH_3	−0.17	4.461	4.460	0.9998
CH_2CH_3	−0.15	4.467	4.472	1.0012
H	0	4.448	4.563	1.0258
F	0.06	4.625	4.599	0.9944
Cl	0.23	4.652	4.703	1.0108
Br	0.23	4.693	4.703	1.0021
COOH	0.45	4.824	4.836	1.0025
NO_2	0.78	5.096	5.036	0.9882

[a] Least-squares best-fit line corresponds to the following equation: "corrected"(HOMO) = σ(0.6067) + 4.5630, for which R = 0.96. [b] In units of eV. [c] Correction factor = ["corrected"(HOMO energy)]/["as is"(HOMO energy)].

distributed over the benzamide's delocalized π system (Figure 14).

In an effort to demonstrate this effect quantitatively, we constructed a plot (Figure 15) of k_3 versus the change in the dipole moment, $\Delta\mu$, for the benzyl portion (as illustrated in Figure 16) of the substrates before versus after attack. In this context, the dipole moment of the benzyl moiety was estimated using Chem-X[21] on the basis of the AM1-optimized charge distribution and structural geometry. By subtracting out the dipole moment before attack, we hoped to remove the normal variation in dipoles among these substituted rings and look only at the change due to increasing electron density on the ring after the attack. This plot (Figure 15) produced another strong correlation (R = 0.96). Still we sought to elucidate more precisely the mechanism by which the charge delocalization operated. These considerations led us to contemplate the possibility that orbital interactions, and specifically HOMO–LUMO interactions, were affording the through-space conduit by which charge was transferred from the reaction site to the benzamide ring system.

Evidence for Orbital Interactions in the Charge Delocalization Mechanism. The role of orbital interactions in reaction schemes has been a prevalent theme in current published literature.[35-43]

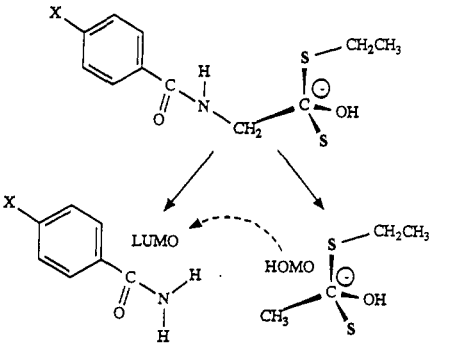

Figure 17. Illustration showing construction of "fragment molecules" from a model compound.

Even prior to this recent surge of interest, workers[44-46] attributed allosteric kinetic effects to interactions involving the frontier orbitals. They also noted that substitution of the benzene ring with electron-withdrawing groups lowered the energies of both the HOMO and LUMO, while substitution with electron-donating groups raised both. These examples served to stimulate our interest in the prospect that the charge delocalization mechanism postulated for these reactions might in fact be mediated by orbital (e.g., HOMO–LUMO) interactions.

During the course of attack by the base-assisted water nucleophile on the acylated enzyme, a negative charge builds on the reaction center in general and on the thiono sulfur [(=S)] in particular. The acyl–enzyme bond [C(=S)--S] weakens and breaks as this charge density shifts to the thiol sulfur. In contemplating the possible role of orbital interactions in this process, we questioned whether the enzyme might be lowering activation energies (and thus providing its catalytic effects) by dispersing electron density from the HOMOs associated with the reaction site into the LUMOs associated with the substituted benzamide moiety. We reasoned that the extent of the HOMOs → LUMOs charge transfer would depend in part on the proximity in energy between the HOMO and LUMO.[35-46] According to this scheme, the role of strong electron-withdrawing groups would be to reduce the HOMO–LUMO energy gap, Δ(LUMO − HOMO). By so doing, these groups would facilitate charge delocalization and hence accelerate deacylation kinetics. The magnitude of Δ(LUMO − HOMO) would then be expected to correlate with the Hammett σ of the substituent group. More indicatively, it should correlate with variations in the reaction's activation energy (as estimated in our calculations by $\Delta(\Delta H_f)$) subject to modulation by the substituent.

To test this premise, we constructed a plot of Δ(LUMO − HOMO) versus $\Delta(\Delta H_f)$. These particular HOMO and LUMO energies were obtained in the following manner. The AM1-optimized structure of the tetrahedral intermediate for each model

(35) Gleiter, R.; Schäfer, W. *Acc. Chem. Res.* **1990**, *23*, 369.
(36) Glauser, W. A.; Raber, D. J.; Stevens, B. *J. Comput. Chem.* **1988**, *9*, 539.
(37) Bacaloglu, R.; Blasó, A.; Bunton, C. A.; Ortega, F. *J. Am. Chem. Soc.* **1990**, *112*, 9336 and pertinent references cited therein.
(38) Basu, G.; Kubasik, M.; Anglos, D.; Secor, B.; Kuki, A. *J. Am. Chem. Soc.* **1990**, *112*, 9410. Kuki, A.; Wolynes, P. G. *Science* **1987**, *236*, 1647. Closs, G. L.; Calcaterra, L. T.; Green, N. J.; Penfield, K. W.; Miller, J. R. *J. Phys. Chem.* **1986**, *90*, 3673. Beratan, D. N.; Onuchie, J. N.; Hopfield, J. J. *J. Chem. Phys.* **1987**, *86*, 4488.
(39) Fujimoto, H. *Acc. Chem. Res.* **1987**, *20*, 448 and references cited therein. Fujimoto, H.; Koga, N.; Fukui, K. *J. Am. Chem. Soc.* **1981**, *103*, 7452.
(40) Fukui, K. *J. Phys. Chem.* **1970**, *74*, 4161. Fukui, K. *Theory of Orientation and Stereoselection*; Springer-Verlag: Berlin, 1975.
(41) Woodward, R. B.; Hoffmann, R. *The Conservation of Orbital Symmetry*; Academic: New York, 1970.
(42) Parr, R. G.; Yang, W. *J. Am. Chem. Soc.* **1984**, *106*, 4049.
(43) Fujimoto, H.; Fukui, K. In *Chemical Reactivity and Reaction Paths*; Klopman, G., Ed.; Wiley-Interscience: New York, 1974; pp 23–54.
(44) Fleming, I. *Frontier Orbitals and Organic Reactions*; Wiley: London, 1976.
(45) Sustmann, R. *Pure Appl. Chem.* **1974**, *40*, 569.
(46) Henri-Rousseau, O.; Texier, F. *J. Chem. Educ.* **1978**, *55*, 437 and references cited therein.

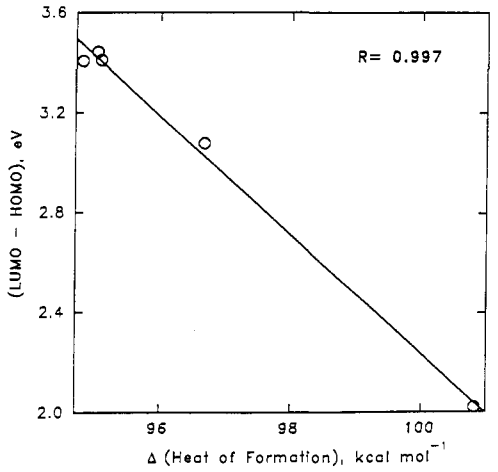

Figure 18. Plot of the Δ(LUMO − HOMO) energy versus $\Delta(\Delta H_f)$.

compound in the series was broken into two "fragment molecules", after which the ends were capped with H atoms. This procedure of constructing our fragment molecules is illustrated in Figure 17. Separate SCF calculations were then run on both molecules so constructed. In these particular AM1 calculations, we made no attempt to achieve geometry optimization or energy minimization. This was deliberate inasmuch as we sought an SCF energy for the fragment molecules in their predetermined conformations. A value for Δ(LUMO − HOMO) was then taken as the difference in energy between the LUMO for the benzamide's fragment molecule and the HOMO for the dithioacyl tetrahedral intermediate's fragment molecule. The resulting plot of Δ(LUMO − HOMO) versus $\Delta(\Delta H_f)$ for the present series of model compounds is given in Figure 18. The correlation coefficient R was an impressive 0.997!

We believe that these results confirm that AM1 discerns a difference in activation energies across this series of model compounds. They also suggest that this difference can be interpreted on the basis of interactions between the orbitals associated with the reaction site and those associated with the benzamide portion of the substrate, in particular their respective HOMOs and LUMOs. Lastly, we assert that the foregoing analysis provides credible evidence that this through-space orbital interaction provides a conduit for electron delocalization during the deacylation step.

Electrostatic and Polarization Effects in Enzyme Catalysis. Our ultimate goal is to provide new insight into the catalytic activity of cysteine proteases. We have proposed here that catalytic effects are gained from the stabilization of the rate-limiting enzyme-bound anionic transition state via a through-space orbital charge delocalization mechanism. Our theoretical studies on dithio ester model compounds have provided compelling evidence for such a mechanism.

We recognize that the kinetics of these reactions is likely not dependent solely on the proposed charge delocalization mechanism. Clearly, other driving and controlling forces are expected to play an important role in so complex a process as an enzymatic reaction.[1-4,47-58] Indeed, a great deal of attention has been paid in recent years to the way in which electrostatic interactions in the active site may lower activation energies of substrates or stabilize activated, zwitterionic forms of the enzyme. For example, Warshel[49,57,58] has proposed that, if an enzymatic reaction experiences large contributions from ionic resonance forms, then the activation energies may be lowered by interactions with the enzyme's active-site dipoles. This is analogous to the stabilization of solvated ions in water or by other highly polar solvents. Distinctively, the enzyme has evolved in such a way so as to orient and fix its dipoles in optimal positions for promoting the catalytic reaction. With regard to the present series of substrates, the possibility that the amide dipole interacted with the thiol sulfur in this fashion was mentioned in a paper by Carey and Storer.[9]

The important role of electrostatic and polar interactions in lowering activation energies in enzymes is hardly disputed.[1-4,47-58] Nevertheless, large, highly polarizable atoms such as sulfur would seem to be less efficient at lowering energy through this mechanism. For example, O–H···S hydrogen bonds are much weaker than O–H···O hydrogen bonds. At the same time, atoms such as sulfur possess large, diffuse orbitals that appear to be ideal donors of HOMO electrons into accessible LUMOs.[35-44] In view of the large buildup of charge density on the S atoms in the present examples, this mechanism may assume considerable importance in lowering activation energies.

A further source of electrostatic stabilization energy may be derived from the oriented dipoles of the hydrogen-bonded backbone groups of an α-helix. This concept has been elaborated by several workers,[50-55] e.g., Hol[51,52] and Pickersgill et al.[54,55] With respect to papain, its catalytic site is located close to the N-terminus of a long α-helix spanning residues 24–42.[1-4] Hol[51,52] has described how the electrical dipole of this α-helix is thought to create an electrical field in the active site which would be beneficial for catalysis by stabilizing both deprotonation of the SH nucleophile and formation of the tetrahedral intermediates. Conversely, Pullman and co-workers[53] have provided theoretical evidence which indicates that the role of the α-helix in proton transfer from Cys-25 to His-159 is superseded by that played by neighboring residues such as Asp-158.

Other aspects of the role of electrostatic and binding interactions in papain's reactivity have been proposed and debated. In a recent study, for example, Pickersgill et al.[54] mapped the electrostatic field of papain by calculating the potential from Poisson's equation. In particular, they focused on the electrostatic properties that govern formation of the thiolate–imidazolium [S^-···H–Im^+] ion pair in the active site. Of course, this step precedes the formation of the tetrahedral intermediate in acylation. They concluded that formation of the thiolate ion (via transfer of the SH proton to the imidazole group of His-159) was promoted by the oriented dipole of the nearby α-helix composed of residues 24–42. A later communication by Brocklehurst et al.[55] disputed the dominant role played by electrostatic effects as contended by Pickersgill et al.;[54] they argued instead that the catalytic-site reactivity of papain was determined by a complex interplay of electrostatic effects as well as conformational contributions and binding interactions. Very recently, Kollman and his co-workers[48] performed a combined molecular mechanics and molecular orbital simulation of the attack by papain's Cys-25 thiol sulfur on substrates during acylation. They concluded that nucleophilic attack by the thiolate ion was either preceded by or coincident with proton transfer from His-159 to the oxygen or nitrogen atom in the scissile peptide group. The Kollman "concerted" model for this initial step of the enzymatic reaction invites revision of the "sequential" models proposed by others.[1]

It is clear from the above discussion that a consensus of opinion on the precise catalytic mechanism followed by the cysteine proteases and related enzymes remains elusive. Perhaps the only conclusion one can draw from the aforementioned discussion is that both electrostatics and binding participate to some degree

(47) Merz, K. M.; Hoffman, R.; Dewar, M. J. S. *J. Am. Chem. Soc.* **1989**, *111*, 5636.
(48) Arad, D.; Langridge, R.; Kollman, P. A. *J. Am. Chem. Soc.* **1990**, *112*, 491.
(49) Warshel, A. *Acc. Chem. Res.* **1981**, *14*, 284.
(50) Wada, A. *Adv. Biophys.* **1976**, *9*, 1.
(51) Hol, W. G. J.; van Duijnen, P. Th.; Berendsen, H. J. C. *Nature* **1978**, *273*, 443. Hol, W. G. J.; Halie, L. M.; Sander, C. *Ibid.* **1981**, *294*, 532.
(52) For a review, see: Hol, W. G. J. *Adv. Biophys.* **1985**, *19*, 133.
(53) Lavery, R.; Pullman, A.; Wen, Y. K. *Int. J. Quantum Chem.* **1983**, *24*, 353.
(54) Pickersgill, R. W.; Goodenough, P. W.; Sumner, I. G.; Collins, M. E. *Biochem. J.* **1988**, *254*, 235.
(55) Brocklehurst, K.; O'Driscoll, M.; Kowlessur, D.; Phillips, I. R.; Templeton, W.; Thomas, E. W.; Topham, C. M.; Wharton, C. W. *Biochem. J.* **1989**, *257*, 309. Pickersgill, R. W.; Sumner, I. G.; Collins, M. E.; Goodenough, P. W. *Ibid.* 310.
(56) Fastrez, J. *Eur. J. Biochem.* **1983**, *135*, 339.
(57) Warshel, A. *Proc. Natl. Acad. Sci. U.S.A.* **1978**, *75*, 5250.
(58) Warshel, A. *Biochemistry* **1981**, *20*, 3167.

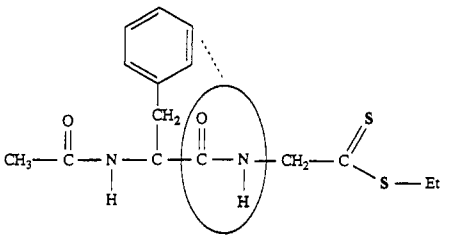

Figure 19. *N*-Acetylphenylalanylglycine dithio ester model compound, illustrating a possible through-space π interaction.

in affording the catalytic effect. At the same time, the importance of the oriented dipole of the α-helix of papain in the catalytic process remains a topic of debate.[50-55] Regardless of these controversies, the theoretical basis for our proposed mechanism does nothing to vitiate the role of electrostatic and binding interactions in the catalytic process. Our interpretation may well prove to merely "expand" the definition of electrostatics and binding effects to include their manifestation through orbital interactions of the type proposed herein. Ultimately, we may discover that catalysis is achieved in these enzymes by the concerted and even synergistic interplay of electrostatics, binding, and orbital interactions.

Concluding Remarks

It may seem peculiar to describe HOMO–LUMO interactions between molecular orbitals on one part of a molecule and molecular orbitals on another part of the same molecule. After all, these orbitals are "molecular". However, in the case of the model compounds under study (Figure 4), they are separated by filled C–C and C–N σ bonds which are highly localized in character. They are thus insulators toward the migration of electron density from one portion of the molecule to the other. In this context, our interpretation represents an extension of the orbital-related arguments expounded by other workers[44-46] to explain a variety of kinetic phenomena. Therefore, an enzyme mechanism that lowers activation energies by dispersing electron density into the LUMOs of a substituted benzamide should be expected to exhibit a strong correlation between the kinetic rate constant k_3 and the Hammett σ of the substituent. Such is exactly the case in the present series of compounds under study.

An alternative (and in a frontier orbital sense, stricter) interpretation of the phenomenon might be to propose that the orbitals of the benzamide portion of the substrate perturb the energy of the dithio ester portion of the substrate. The energy of the LUMOs of the substrate is thereby lowered, rendering the interaction with the HOMOs of the attacking water nucleophile more facile. It is our opinion, however, that the differences in these interpretations are chiefly semantic.

The most important specificity in papain's cleavage of protein substrates is its preference for phenylalanine residues in the S2 subsite.[1-4] This is the binding site for the amino acid residue once removed from the cleavage site, toward the N-terminus of the substrate. What significance, if any, this has in the context of our current work remains obscure. Nevertheless, there is a discernible structural homology between *N*-acetylphenylalanylglycine dithioacyl papains (Figure 19) and the model compounds considered in this study (see Figure 4). In contrast to the model compounds under study, the phenyl ring in the phenylalanyl dipeptide is not directly conjugated to the amide; rather, it is bonded to an sp^3 carbon. This is of course the case for all peptide bonds in proteins. Yet k_3 is faster for the phenylalanyl dipeptide than for *N*-benzoylglycine papain.[59]

It is evident that in an enzyme, where many groups of atoms are held in close proximity to one another, many sets of orbitals will interact and perturb one another. Thus, the thiol sulfur may interact with the LUMO of the peptide bond while both are also interacting with the LUMOs of the phenyl ring of the substrate phenylalanine (Figure 17) and with other low-energy unoccupied orbitals in the active site. The cumulative effect of such interactions could be a significant lowering of activation energies. Bürgi et al.[30] describe the attacks of nucleophiles on carbonyls as proceeding through five steps: (1) approach of the nucleophile, (2) passage through the first transition state, (3) formation of a tetrahedral intermediate, (4) passage through a second transition state, and (5) the formation of products. In this context, it is interesting to speculate whether a phenylalanine residue in the S2 subsite might be the perfect compromise in terms of lowering the activation energy (step 2) without overstabilizing the tetrahedral intermediate (step 3), which could otherwise slow the reaction.

In the present study, we have carried out a series of semiempirical and ab initio molecular orbital calculations on a series of dithio ester model compounds for which experimental data abound. Our goal was to relate the crystallographic structures of these molecules and the implied configurations of the enzyme–substrate intermediates to the minimum-energy conformations derived computationally for these model compounds. In addition, we sought to identify structural and electronic parameters that affect the kinetics of deacylation and which may illuminate its mechanism. We concentrated on the energy of the anionic tetrahedral intermediate as opposed to the entire reaction energy profile. As a local energy minimum, this intermediate is more conducive to analysis by AM1 than the precise path followed by the reacting molecule across the energy hypersurface. Dewar has alluded to this issue in determining AM1 activation energies.[13] In light of the Hammond postulate,[60] we expect a great deal of similarity between the structure of the tetrahedral intermediate and that of the transition state. Therefore, it appears reasonable to assume that factors which lower the energy of the anionic tetrahedral intermediate will lower the energy of the transition state proportionally. At the present time, we are generating full AM1 reaction energy profiles for these substrates. Such implementations of AM1 have proved useful in recent studies of other reactions.[33,47,48,61-63]

While the focus of this paper is on the dithio ester intermediates, we have no reason to doubt that the effects described herein would be just as important for the biological system, in which case the intermediate is a thiol ester. In fact, the absence of a second sulfur atom in the thiol ester [C(=O)—S] case will result in a greater amount of electron density being pushed into the C—S antibonding orbitals, perhaps making its dispersion through this type of mechanism even more important. Interestingly, normal ester substrates forming thiol ester intermediates have been found to display similar kinetic effects with ring substituents.[5-11,59]

Acknowledgment. The authors extend their gratitude to the National Science Foundation, which has supported this work through the award of two NSF-Research Experiences for Undergraduates fellowships to G.D., to the University of Missouri—St. Louis for the use of its computational facilities, to Drs. Andrew Storer and Paul Carey of the National Research Council of Canada for their suggestions, and to Biosym Technologies, Inc., for use of their programs InsightII and Discover. Finally, the authors are indebted to the reviewers of this paper for offering several helpful suggestions.

(59) Hammond, G. S. *J. Am. Chem. Soc.* **1955**, *77*, 334.

(60) Dewar, M. J. S.; Yuan, Y.-C. *J. Am. Chem. Soc.* **1990**, *112*, 2088. *Ibid.* 2095.

(61) Katagi, T. *J. Comput. Chem.* **1990**, *11*, 524.

(62) Bacaloglu, R.; Bunton, C. A.; Ortega, F. *J. Am. Chem. Soc.* **1989**, *111*, 1041. Bacaloglu, R.; Blasko, A.; Bunton, C. A.; Ortega, F. *Ibid.* **1990**, *112*, 9336.

(63) Tonge, P. J.; Lee, H.; Sans Cartier, L. R.; Ruzsicka, B. P.; Carey, P. R. *J. Am. Chem. Soc.* **1989**, *111*, 1496.